

ARTICLES

Photophysical Studies of Porphyrins and Metalloporphyrins: Accurate Measurements of Fluorescence Spectra and Fluorescence Quantum Yields for Soret Band Excitation of Zinc Tetraphenylporphyrin**Jerzy Karolczak,^{*,†,‡} Dorota Kowalska,[§] Adam Lukaszewicz,[§] Andrzej Maciejewski,^{‡,||} and Ronald P. Steer^{*,⊥}**

Faculty of Physics, A. Mickiewicz University, Umultowska 85, 61–614 Poznan, Poland, Faculty of Chemistry, A. Mickiewicz University, Grunwaldzka, 60-780 Poznan, Poland, Center for Ultrafast Laser Spectroscopy, A. Mickiewicz University, Umultowska 85, 61-614 Poznan, Poland, and Department of Chemistry, University of Saskatchewan, 110 Science Place, Saskatoon, Saskatchewan, Canada S7N 5C9

Received: January 8, 2004

For the test system zinc tetraphenylporphyrin in ethanol, the S_2-S_0 and S_1-S_0 absorption and emission spectra and fluorescence quantum yields have been measured as a function of excitation wavelength within the Soret and Q-bands under conditions where self-absorption of emission and solute aggregation are either eliminated or properly compensated. Under these conditions, the smallest S_2-S_0 Stokes shift yet measured, 115 cm^{-1} , and the largest S_2-S_0 absolute fluorescence quantum yield yet measured, 1.84×10^{-3} , are obtained. Accurate measurements of the relative quantum yields of S_2-S_0 to S_1-S_0 emission as a function of excitation wavelength reveal that a fast radiationless process that bypasses S_1 is operative among states accessed at excitation energies that span the Soret band. The data can be interpreted using the evidence of Yu, Baskin, and Zewail that a second excited state, S_2' , contributes a small fraction of the Soret band's integrated molar absorptivity and is responsible for an increasing fraction of photon absorption on both the red edge of the Soret band at $\lambda_{\text{ex}} > 430\text{ nm}$ and the blue at $\lambda_{\text{ex}} < 409\text{ nm}$. The lifetimes of the S_2 and S_1 states have also been measured under similar conditions; the values obtained confirm previous measurements.

Introduction

Porphyrins, metalloporphyrins, and related molecules have assumed extraordinary importance in recent years as the opportunities for using these compounds in photodynamic therapy,¹ optoelectronic devices,² sensors,³ molecular logic devices,⁴ and artificial solar energy harvesting and storage schemes⁵ have become apparent. Studies of the spectroscopy and photophysical dynamics of these compounds and their multichromophoric derivatives have grown exponentially in number in the last 10 years. During this period, increasing attention has been paid to the behavior of higher electronic states accessed by pumping in the strong Soret absorption band located in the violet region of the spectrum. Of particular note are recent studies⁶ showing that electron transfer can occur on a picosecond time scale from these upper excited state(s) in zinc tetraphenylporphyrin (ZnTPP) to solvents such as dichloromethane. Very recently, Yu, Baskin, and Zewail⁷ (hereafter referred to as YBZ) confirmed and elaborated upon this observation and provided the first evidence that heretofore undiscovered electronic states may be involved in the relaxation of ZnTPP excited by one-photon absorption in the Soret bands. (For consistency,

we use S_2' to label the new singlet state identified by YBZ, and S_1 and S_2 to label the states populated by absorption in the Q and B (Soret) bands.)

Metalloporphyrins present many challenges to those who would measure accurate, artifact-free spectra, emission quantum yields and temporal decay profiles, particularly when probing the UV-blue region. First, owing to their rigid structure, the metalloporphyrins exhibit Stokes shifts of at most a few hundred wavenumbers between the maxima of their S_2-S_0 absorption and emission bands; overlap of the absorption and emission spectra is therefore substantial. Coupled with the huge oscillator strength of the Soret absorption ($\epsilon_{\text{max}} \approx 5 \times 10^5\text{ M}^{-1}\text{ cm}^{-1}$), this overlap results in extensive reabsorption of emission, making it difficult to measure undistorted fluorescence spectra and to obtain S_2-S_0 fluorescence quantum yields with the usual accuracy of a few percent. Reabsorption can also lead to artifacts in the measurement of temporal emission and transient absorption spectra and decay constants.

In addition, many porphyrins and metalloporphyrins readily aggregate, making it difficult to extract the behavior of monomeric species from measurements on solutions containing mixtures of monomer, dimer, and higher aggregates. The nature of the aggregate can vary with the nature of the porphyrin solute, the solvent, the temperature, and the presence of surfactant, electrolyte, or other solution additives.^{8–10} Aggregation occurs at micromolar porphyrin concentrations in some systems and

[†] Faculty of Physics, A. Mickiewicz University.

[‡] Center for Ultrafast Laser Spectroscopy, A. Mickiewicz University.

[§] Faculty of Physics and Faculty of Chemistry, A. Mickiewicz University.

^{||} Faculty of Chemistry, A. Mickiewicz University.

[⊥] Department of Chemistry, University of Saskatchewan.

is therefore impossible to avoid when working at the higher solute concentrations needed for most transient absorption^{7,11} and fluorescence up-conversion^{7,12} measurements.

Additional problems (or opportunities) include multiple-photon absorption, a process that is significant even at very low metalloporphyrin concentrations when high peak power picosecond or femtosecond lasers are used as excitation sources. Excitation of somewhat more concentrated solutions with such lasers may also produce excited electronic state densities that are large enough to result in significant bimolecular excited-state annihilation,¹³ a source of delayed fluorescence from S_1 and T_1 states.

Most previous work to characterize the structure and relaxation dynamics of the upper excited states of the metalloporphyrins has relied on standard measurements of fluorescence spectra, quantum yields, and lifetimes.^{14,15} In particular, transient absorption and fluorescence upconversion measurements have most often been made at solute concentrations in which aggregation was an unavoidable complication.^{11,12,16} This paper seeks to characterize the upper excited state relaxation dynamics of monomeric ZnTPP, a well-studied metalloporphyrin, by providing reliable, artifact-free fluorescence spectra and fluorescence quantum yield and fluorescence lifetime measurements on highly dilute solutions. To do so, we employ an improved time-correlated single-photon counting method to measure reproducible fluorescence lifetimes with subpicosecond temporal resolution. We also describe in detail a procedure to obtain undistorted S_2 - S_0 emission spectra and accurate S_2 fluorescence quantum yields following excitation of highly dilute solutions in the Soret band.

Experimental Section

Materials. 5,10,15,20-Tetraphenyl-21*H*,23*H*-porphine zinc (ZnTPP) of the highest purity (Aldrich, low chlorin) was used as received. Ethanol for spectroscopy (Merck), hexane for fluorescence (Merck), and tetrahydrofuran for fluorescence (Merck) were used as received. For comparison we also used ethanol from a second source (Aldrich, HPLC grade), which was additionally purified by fractional distillation and dried.

Methods. The picosecond laser excitation and time-correlated single-photon counting detection systems used to measure fluorescence lifetimes with subpicosecond precision have been described in detail previously.¹⁷ Briefly, the train of 1–2 ps pulses from an argon ion-pumped, tunable, mode-locked Ti:sapphire laser was pulse-picked at a frequency ranging from single shot to 4 MHz. Second and third harmonics of these pulses were used as the excitation source for the measurement of upper state fluorescence lifetimes by time-correlated single-photon counting. A graded, rotating neutral density filter was used to control the intensity of the excitation beam and a Fresnel double rhomb was employed to rotate the plane of its polarization. Together with a polarizer set to observe emission at the magic angle, this arrangement eliminates rotational diffusion artifacts. The detector is a Hamamatsu R3809U-05 microchannel plate photomultiplier.

The same excitation system, which is based on a modified Edinburgh Instruments FL 9000 spectrofluorometer, was also used to excite samples in measurements of their S_2 - S_0 fluorescence spectra and fluorescence quantum yields. In these experiments, the excitation beam was directed into a thin cell with a 0.5–1.0 mm excitation path length, and was focused mildly with a quartz lens to a point close to the front wall of the cell, from which emission was observed. The beam diameter at the beam focus was no more than 0.5 mm (and could be as

small as 0.1 mm), so that the path length for reabsorption of S_2 - S_0 emission was minimized. With this arrangement, measurable reabsorption of emission could be detected only when ZnTPP concentrations exceeded 2×10^{-6} M. To ensure that a linear relationship was maintained between absorbed intensity and emission intensity, smaller absorption path cells (0.2 or 0.5 mm for concentrations $> 2 \times 10^{-5}$ M) were used when the excitation wavelengths were longer than 415 nm (i.e., when ϵ exceeded ca. $1.6 \times 10^5 \text{ M}^{-1} \text{ cm}^{-1}$) or when higher concentrations of the metalloporphyrin were employed.

The spectral bandwidth of the laser excitation source is narrow (ca. 10 cm^{-1}) and transform-limited. This is unlike the situation found in conventional fluorometers using polychromatic sources and, for quantum yield measurements, permits the sample absorbance at the excitation wavelength to be measured accurately using a UV-visible spectrophotometer employing the same (small) spectral bandwidth. This is particularly important in determining quantum yields when exciting on the steep slopes of the Soret absorption band. The spectral bandwidth employed for the emission monochromator was ca. 0.9 nm (or ca. 50 cm^{-1}) at the maximum of the S_2 - S_0 emission spectrum, enabling a determination of the relatively distortion-free shape of the S_2 - S_0 emission spectrum even though the main band is very narrow (fwhm $\sim 430 \text{ cm}^{-1}$). The overall system permitted emission measurements to begin at a wavelength only 2 nm to the red of the excitation wavelength.

The following detailed procedure was followed to obtain emission quantum yields and spectra that were undistorted and changed only in relative intensity with changing solute concentration and excitation wavelength within the Soret band. To obtain a quantitative measure of the relative intensity of the exciting light, the fluorescence intensity of an approximately 10^{-5} M solution of rhodamine B in ethylene glycol, used as a quantum counter, is measured for given excitation and emission wavelengths. The sample emission spectrum is then measured several times under the same conditions, using the short path length cell described above, and the average spectrum is obtained by sequentially adding the digital spectra and finally dividing by the total number of spectra used. The sample is replaced by the rhodamine solution and the relative intensity of the excitation beam is measured again. The emission (and Rayleigh plus Raman scattering) spectrum of a blank (solvent only) is then obtained under conditions identical to those for the sample, and the intensity of the excitation light is checked again using the quantum counter. The noise level is determined by measuring the emission spectrum without the cell present, and the cycle ends with a fourth measurement of the excitation intensity with the rhodamine quantum counter. The noise spectrum is then subtracted from the spectra of both the sample and the blank.

The spectrum of the blank, with noise subtracted, was then corrected for the reduced incident intensity (due to absorption by the sample) at the locus of the emission by multiplying it by the factor $x = (1 - 10^{-A_\lambda})/2.3A_\lambda$ where A_λ is the absorbance of the sample measured at the excitation wavelength. (In the latter measurements the spectral bandwidth of the absorption spectrophotometer was set at ≤ 1 nm to avoid artifacts due to spectral distortion found at larger slit widths.) This corrected spectrum of the noise-subtracted blank is then subtracted from the averaged emission spectrum of the sample. Finally, the solvent-and-noise-subtracted emission spectrum is further corrected for the sensitivity of the detection system, using the emission correction files supplied by the spectrometer manufacturer. These spectra are then normalized to account for

different relative intensities of the exciting light at the various excitation wavelengths, $I_0(\lambda_{\text{ex}})$, as measured by the rhodamine quantum counter. They are further normalized to account for differences in the intensity of the incident light absorbed by the sample at the different excitation wavelengths, $I_a(\lambda_{\text{ex}})$, as determined from a quantitative measurement of A_λ in the absorption spectrum. The resulting S_2-S_0 emission spectra were identical in shape for several excitation wavelengths and differed only in relative integrated intensity, by a factor directly proportional to the relative emission quantum yield, $\phi_{\text{f,rel}}$, at each excitation wavelength. Absolute emission quantum yields were then obtained conventionally by using a quinine sulfate in 0.05 M aqueous H_2SO_4 ($\phi_{\text{f}} = 0.52$) as a reference standard¹⁸ and applying the same procedure to it and the sample.

The above procedure was all that was necessary to obtain undistorted, artifact-free S_2-S_0 emission spectra at the lowest metalloporphyrin concentrations ($<2 \times 10^{-6}$ M in ethanol), where the dimer contributed negligibly to the absorption spectrum in the region of the Soret band, and reabsorption of emission by the monomer was less than 2% owing to the use of thin samples and very small reabsorption path lengths. At higher porphyrin concentrations, significant reabsorption was unavoidable, and a further correction of the emission spectrum was employed to account for this systematic error. This correction involved calculation of the constant effective reabsorption path length, l_{em} , needed to make the shape of the corrected emission spectrum independent of the concentration of the porphyrin and identical to those from samples of low concentration containing negligible dimer. The uncertainty in l_{em} was estimated to be <0.05 mm, so that reabsorption will introduce a systematic error in the absolute emission quantum yields of no more than 5% at the highest porphyrin concentrations employed in the present study.

Quantum yields of relatively intense S_1-S_0 fluorescence, excited in either the S_2-S_0 or S_1-S_0 absorption systems, were determined routinely using a modified MPF-3 spectrofluorometer (Perkin-Hitachi) as previously described.¹⁹ The values of these quantum yields agreed well with those obtained nonroutinely using the laser excitation source, thin cell, and correction process described above for obtaining S_2-S_0 fluorescence quantum yields.

Results and Discussion

Figure 1 shows the S_2-S_0 absorption and corrected emission spectra of ZnTPP in ethanol obtained as described above. Note that the S_2-S_0 absorption and corrected emission spectra are nearly perfect mirror images, and that the Stokes shift is very small, $115 \pm 15 \text{ cm}^{-1}$, as expected of a rigid metalloporphyrin embedded in a solvent in which reorganization on excitation has only a minor effect. This value of the S_2-S_0 Stokes shift is the smallest ever reported for ZnTPP in any solvent at room temperature. Note, in contrast, the differences between similar absorption and emission spectra reported by Mataga et al., in which the precautions for obtaining artifact-free spectra noted above were not taken.¹⁶ We expect that the wide range of values of the Stokes shift and quantum yield of S_2-S_0 emission for the same metalloporphyrin in the same or similar solvents reported to date is due primarily to the failure to satisfactorily account for emission reabsorption in these measurements, and secondarily to the effects of dimerization and scattering. Such errors in the measurement of quantum yields are propagated in calculations of S_2 lifetimes using $\tau_{\text{f}} = \phi_{\text{f}}/k_{\text{f}}$, where the radiative rate constant, k_{f} , can be estimated accurately from the integrated molar absorptivity of the Soret absorption band. Calculations

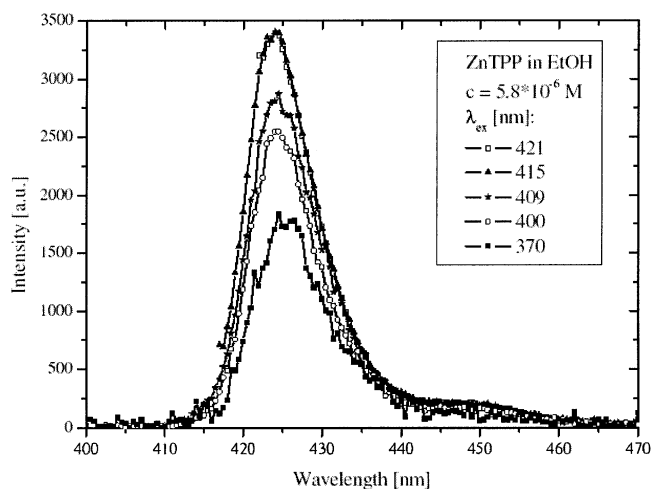


Figure 1. S_2-S_0 emission spectra of ZnTPP ($c = 5.8 \times 10^{-6}$ M) in ethanol at room temperature as a function of excitation wavelength. The spectra have been corrected for differences in absorbance and intensity of excitation at the several excitation wavelengths and for reabsorption.

of the sum of the rate constants for nonradiative decay of the S_2 state, Σk_{nr} , using the expression $\Sigma k_{\text{nr}} = (1 - \phi_{\text{f}})/\tau_{\text{f}}$ will contain little error due to large errors in measuring ϕ_{f} because $\phi_{\text{f}} \ll 1$ but will be inaccurate if τ_{f} is in error. The importance of reabsorption in quantitative measurements of S_2-S_0 emission intensities and spectral parameters has been identified and accounted for by YBZ;⁷ nevertheless, we obtain a significantly smaller Stokes shift than they report (115 cm^{-1} vs 300 cm^{-1} in benzene).

With the ability to record artifact-free S_2-S_0 emission spectra and quantum yields in hand, it is then possible to determine the quantitative photophysical effects of changing the excitation wavelength, λ_{ex} , within the Soret band system. Such measurements are particularly important because many previous investigators have chosen to excite at wavelengths well to the blue of λ_{max} to avoid scattering when λ_{ex} is close to λ_{em} . Many investigators have assumed that the photophysics of this metalloporphyrin is essentially independent of λ_{ex} within the spectrally narrow Soret band system, but the recent experiments of YBZ cast serious doubt on that assumption.

First, the corrected, normalized emission spectrum is completely independent of excitation wavelength within the range $370 \text{ nm} < \lambda_{\text{ex}} < 421 \text{ nm}$, as illustrated in Figure 2. YBZ have suggested that another state, S_2' , is present and absorbs significantly in the same region. These results suggest that S_2' , if present, has almost the same emission spectrum as S_2 and/or exhibits a substantially lower fluorescence yield than S_2 . The results of our measurements of the relative quantum yields of both S_2-S_0 and S_1-S_0 fluorescence as a function of λ_{ex} in the Soret system at several low ZnTPP concentrations are shown in Table 1. The effects of increasing the concentration of ZnTPP on these S_2-S_0 and S_1-S_0 fluorescence quantum yields at constant $\lambda_{\text{ex}} = 409 \text{ nm}$ are shown in Table 2.

The numbers in Tables 1 and 2 are $\phi_{\text{f,rel}} = \phi_{\text{f}}(\lambda_{\text{ex}}, c)/\phi_{\text{f}}(\lambda_{\text{ex}} = \lambda_{\text{ref}}, c = c_{\text{ref}})$ and are obtained from the integrated intensities of the corrected emission spectra, as described above. We estimate that the error in these values of $\phi_{\text{f,rel}}$ is about 5%. The reference solutions contain ZnTPP at concentrations where dimer formation is negligible, so any variations in $\phi_{\text{f,rel}}$ are due to real photophysical effects involving the monomer or, at higher solute concentrations, to the formation of aggregates.

The absolute quantum yield of S_2-S_0 fluorescence for ZnTPP in ethanol (concentrations $c \leq 5.8 \times 10^{-6}$ M) excited at $\lambda_{\text{ref}} =$

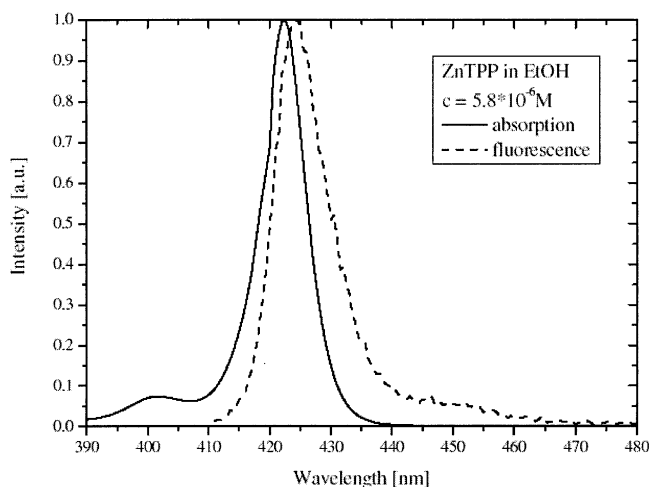


Figure 2. S_2 – S_0 absorption and normalized corrected emission spectra of ZnTPP in ethanol at room temperature. The emission spectrum was obtained at an excitation wavelength of 415 nm.

TABLE 1: Relative Quantum Yields of S_2 – S_0 and S_1 – S_0 Fluorescence of Monomeric ZnTPP in Ethanol as a Function of λ_{ex} in the Soret Band at Room Temperature

λ_{ex} (nm)	$\phi_{\text{f,rel}}(S_2-S_0)^a$	$\phi_{\text{f,rel}}(S_1-S_0)^a$
370	0.60	0.76
400	0.77	0.83
409	0.88	0.89
415 ^b	1.00	1.00

^a Average of measurements at $c = 1.8 \times 10^{-6}$ M and $c = 5.8 \times 10^{-6}$ M. ^b Excitation wavelength used for normalization.

TABLE 2: Relative Quantum Yields of S_2 – S_0 and S_1 – S_0 Fluorescence of ZnTPP in Ethanol as a Function of ZnTPP Concentration for $\lambda_{\text{ex}} = 409$ nm

c (μM)	$\phi_{\text{f,rel}}(S_2-S_0)$	$\phi_{\text{f,rel}}(S_1-S_0)$
0.44		1.02
1.8 ^a	1.00	1.00
5.8	1.00	0.98
31	0.78	
140	0.58 ^b	

^a Concentration used for normalization. ^b Correction very large and value more uncertain.

415 nm is determined by us to be $\phi_{\text{f}} = 1.84 \times 10^{-3}$. This number may be used to obtain good estimates of the absolute S_2 fluorescence quantum yields from the data in Table 1, but these absolute quantum yields will be subject to greater error than $\phi_{\text{f,rel}}$.

The data in Table 2 (for which $c_{\text{ref}} = 1.8 \times 10^{-6}$ M and small reabsorption effects have been compensated) indicate that there is no significant change in the S_1 – S_0 fluorescence quantum yield at concentrations below 5.8×10^{-6} M and at most a 10% change in the S_2 – S_0 fluorescence quantum yield over the same range. The significantly lower fluorescence quantum yields obtained at still higher concentrations ($c \geq 5.8 \times 10^{-6}$ M, corrected for reabsorption) are, however, significant. We ascribe this observation to the fact that, at these higher concentrations, a significant fraction of the absorption at 409 nm is due to ZnTPP aggregates that exhibit much lower emission quantum yields than the monomer. Note that such higher concentrations ($c \approx 10^{-4}$ M) are often used for fluorescence upconversion or transient absorption experiments.^{11,12,16}

The choice of reference excitation wavelength, 415 nm, was dictated by the wish to excite at a wavelength that was close to the peak of the Soret band at 422 nm, but nevertheless

sufficiently to the blue of λ_{em} to enable most of the emission spectrum to be recorded without interference from scattered excitation light. Several measurements of $\phi_{\text{f,rel}}$ were also made at still longer excitation wavelengths, taking extreme care to ensure that Rayleigh and Raman scattering did not adversely affect the corrected emission spectra. No significant difference was found in the intensity and shape of the corrected S_2 – S_0 emission spectra for excitation in the range $415 \text{ nm} < \lambda_{\text{ex}} < 421 \text{ nm}$, and for several different concentrations in the range $c \leq 5.8 \times 10^{-6}$ M. We therefore conclude that $\phi_{\text{f}} = 1.84 \times 10^{-3}$ for the radiative S_2 – S_0 decay of the monomer in ethanol, when excited at or near $\lambda_{\text{max}} = 422 \text{ nm}$ in the Soret band, and we use this value to obtain absolute values of the rate constants for the radiative and nonradiative rate constants of S_2 . Careful examination of the primary literature reveals that this value of the S_2 – S_0 fluorescence quantum yield is larger than any reported to date for ZnTPP in ethanol or other similar solvents. In particular, the oft-quoted value of $\phi_{\text{f}}(S_2-S_0) = 1.8 \times 10^{-3}$ given by Tsvirko et al.²⁰ is based on a measurement of the relative intensities of S_2 – S_0 : S_1 – S_0 fluorescence and an early measurement²¹ of the absolute value of $\phi_{\text{f}}(S_1-S_0) = 0.03$ for ZnTPP in ethanol, which is too large by about $1/3$. Later measurements by the same authors²² give $\phi_{\text{f}}(S_1-S_0) = 2.2 \times 10^{-2}$ and $\phi_{\text{f}}(S_2-S_0) = 1.1 \times 10^{-3}$; the former value agrees with our present measurement, but the latter is 40% too small, likely due to reabsorption that may be clearly seen in their published emission spectrum. Some tabulated values of $\phi_{\text{f}}(S_2-S_0)$ in the reference literature²³ are systematically too small, by as much as a factor of 5 or 6.

The data in Table 1 show that there is a significant decrease in ϕ_{f} for both S_2 – S_0 and S_1 – S_0 radiative decay as λ_{ex} is moved to the blue within the Soret system, for ZnTPP concentrations at which only monomer is expected to be present in significant amounts. The effect is more pronounced for S_2 – S_0 emission than it is for S_1 – S_0 , i.e., $\phi_{\text{f,rel}}(S_2-S_0)$ is systematically smaller than $\phi_{\text{f,rel}}(S_1-S_0)$ for a given concentration and excitation wavelength, and this difference increases as the excitation energy increases for $\lambda_{\text{ex}} < \lambda_{\text{max}} = 422 \text{ nm}$. Within experimental error, these relative quantum yields are independent of ZnTPP concentration in the range $c \leq 5.8 \times 10^{-6}$ M. We ascribe these observations to (i) an increase in the radiationless decay rates of electronically excited ZnTPP molecules with increasing excitation energy in the Soret region, and (ii) a concomitant increase in the fraction of excited molecules that decay by bypassing S_1 (vide infra).

Although it was impossible to measure accurate S_2 – S_0 fluorescence quantum yields at $\lambda_{\text{ex}} > 421 \text{ nm}$, it was possible to measure $\phi_{\text{f,rel}}$ for S_1 – S_0 fluorescence at λ_{ex} up to 435 nm, using the intensities of S_1 – S_0 fluorescence obtained for direct excitation to S_1 at wavelengths in the Q absorption bands ($\lambda_{\text{ex}} = 555 \text{ nm}$) as a reference. These excitation energies lie well to the red of $\lambda_{\text{max}} = 422 \text{ nm}$ within the Soret band. Table 3 presents the results. Note the dramatic decrease in the quantum yield of S_1 – S_0 fluorescence when the system is excited at wavelengths on the red edge of the Soret band, compared with direct excitation into the Q-bands. This result provides the first direct, unequivocal evidence of the existence of a significant electronic relaxation channel in the upper singlet manifold of ZnTPP that bypasses the S_1 state.

The results of measuring the lifetimes of the S_2 and S_1 states in dilute solution, using the fast time-correlated single-photon counting method previously described, are shown in Table 4. Here $415 \text{ nm} < \lambda_{\text{ex}} < 420 \text{ nm}$, $450 \text{ nm} < \lambda_{\text{em}} < 460 \text{ nm}$ for the S_2 state, $\lambda_{\text{em}} = 650 \text{ nm}$ for the S_1 state, and $c = 4 \times 10^{-6}$

TABLE 3: Relative Quantum Yields of S_1 – S_0 Fluorescence and of Nonradiative Decay for Monomeric ZnTPP in Ethanol at Room Temperature as a Function of λ_{ex} on the Red Side of the Soret Band

λ_{ex} (nm)	$\phi_{\text{f,rel}}(S_1-S_0)^a$	$\Sigma\phi_{\text{nr}}(\text{Soret})^b$
415	1.00 ± 0.00	0.00
424	0.76 ± 0.01	0.24
429	0.52 ± 0.02	0.48
435	0.49 ± 0.02	0.51
555 ^a	1.00	

^a $\phi_{\text{f,rel}}(S_1-S_0) = \phi_{\text{f}}(S_1-S_0, \lambda_{\text{ex}}) / \phi_{\text{f}}(S_1-S_0, \lambda_{\text{ex}}=555 \text{ nm})$. ^b $\Sigma\phi_{\text{nr}}(\text{Soret}) = 1 - \phi_{\text{f,rel}}(S_1-S_0)$ is the sum of the relative quantum yields of nonradiative decay processes when ZnTPP monomer is excited in the Soret region.

TABLE 4: Lifetimes of S_2 – S_0 and S_1 – S_0 Fluorescence and Excited State Decay Constants of Monomeric ZnTPP in Ethanol at Room Temperature; $\lambda_{\text{ex}} = 415 \text{ nm}$ for S_2 and 555 nm for S_1

solvent	$\tau(S_2)^a$ (ps)	$k_{\text{f}}(S_2-S_0)^b$ (s^{-1})	$\Sigma k_{\text{nr}}(S_2)$ (s^{-1})	$\tau(S_1)^a$ (ns)	$k_{\text{f}}(S_1-S_0)^c$ (s^{-1})	$\Sigma k_{\text{nr}}(S_1)^c$ (s^{-1})
EtOH	1.4 ± 0.3 (1.03)	1.31×10^9	7.1×10^{11}	1.88 (1.00)	1.42×10^7	5.14×10^8
THF	1.3 ± 0.3 (0.88)		7.7×10^{11}	1.74 (1.00)		
Hexane				1.96 (1.00)		
Benzene ^d	1.45 ± 0.10		-6.9×10^{11}	1.7		

^a Numbers in parentheses are values of reduced χ^2 for the fit of the data to a single-exponential decay curve. ^b Using $\phi_{\text{f}}(S_2-S_0) = 1.84 \times 10^{-3}$. ^c Using $\phi_{\text{f}}(S_1-S_0) = 2.67 \times 10^{-2}$. ^d Results of YBZ⁷ for one-photon excitation at 397 nm.

M, so we expect that these results characterize the relaxation of the excited monomer of ZnTPP in ethanol. The reduced χ^2 values (Table 4) are obtained from the best fit of a single-exponential decay function to the data, using the iterative reconvolution method described previously. These results may be compared with the results of YBZ,⁷ who obtained $\tau(S_1) = 1.7 \text{ ns}$ and a more precise value of $\tau(S_2) = 1.45 \text{ ps}$ for excitation of dilute solutions of ZnTPP in benzene at 397 nm. These results should also be compared with the value of $\tau(S_2) = 2.35 \text{ ps}$ ^{12,16} obtained at much higher ZnTPP concentrations in ethanol (ca. $1.5\text{--}2.0 \times 10^{-4} \text{ M}$), where extensive dimer formation occurs.

The measured values of $\tau(S_2) = 1.4 \text{ ps}$ and $\phi_{\text{f}}(S_2-S_0) = 1.84 \times 10^{-3}$ then allow us to calculate reliable experimental values of the radiative and nonradiative rate constants for the relaxation of the ensemble of ZnTPP molecules excited in ethanol near the maximum of the Soret band. The results give $k_{\text{f}}(S_2-S_0) = 1.31 \times 10^9 \text{ s}^{-1}$ and $\Sigma k_{\text{nr}}(S_2) = 7.1 \times 10^{11} \text{ s}^{-1}$. A value of k_{f} may also be calculated from the oscillator strength of the Soret bands using the Strickler–Berg formalism.²⁴ The result for ZnTPP in ethanol is $k_{\text{f}} = 1.15 \times 10^9 \text{ s}^{-1}$, in reasonable (but not perfect) agreement with the measurement, giving increased confidence that the measured values of both $\tau(S_2)$ and $\phi_{\text{f}}(S_2-S_0)$ are correct.

The data in Tables 1 and 4 provide the first quantitative evidence of a significant radiationless relaxation process in states $S_{n \geq 2}$ that bypasses S_1 . Note that (i) this nonradiative relaxation process increases in relative importance as the excitation energy increases within the Soret band, and (ii) as this nonradiative process increases in rate (relative to an assumed constant rate of radiative decay), the fraction of nonradiative decay events populating S_1 also decreases. Because electronic relaxation occurs on a time scale that is at least an order of magnitude faster than that of intermolecular vibrational cooling in this system, the $S_{n > 1}$ excited state ensemble will retain a large fraction of any initial vibrational energy possessed by ground

state molecules or acquired by them in photon absorption. (Note, however, that the vibrational energy will be distributed among a larger number of modes due to fs intramolecular vibrational redistribution, IVR, among states of approximately equal energy). These data therefore suggest that either (i) the rate of an additional (as yet unspecified) radiationless decay process increases with increasing S_2 vibrational energy and increasingly bypasses S_1 or (ii) another state, which exhibits a smaller quantum yield of fluorescence in the blue than S_2 and decays by bypassing S_1 , is absorbing an increasing fraction of the light at $\lambda_{\text{ex}} < \lambda_{\text{max}}$.

Second, the data in Table 4 show that excitation on the red edge of the Soret band accesses a radiationless decay path that bypasses S_1 to a still greater extent. If only one electronic transition contributes to the Soret band in the 424–440 nm region, excitation at wavelengths lying progressively further to the red of the absorption maximum will select subsets of the ensemble that contain increasing fractions of vibrationally excited ground-state molecules. Photon absorption therefore produces $S_{n > 1}$ molecules that are either vibrationally cold or vibrationally excited in those low frequency modes that experience a large decrease in vibrational frequency in the excited state. A change in the vibrational characteristics of the excited state ensemble is therefore anticipated as the excitation wavelength moves to the red edge of the Soret band, provided that only one electronic transition is involved. However, radiationless transition theory suggests it is unlikely that an increasing population of either vibrationally cold excited molecules or molecules possessing a nonstatistical distribution of vibrational energies in low-frequency modes could promote a faster rate of radiationless decay via some channel that bypasses S_1 .

On the other hand, the data in both Tables 1 and 4 can readily be interpreted using the evidence presented by YBZ that a second excited state, S_2' , is present, contributes a small fraction of the Soret band's integrated molar absorptivity and is responsible for an increasing fraction of photon absorption on both the red edge of the Soret band at $\lambda_{\text{ex}} > 430 \text{ nm}$ and to the blue at $\lambda_{\text{ex}} < 409 \text{ nm}$.

The strongest evidence supporting this suggestion is provided by YBZ, who made the following important observations for ZnTPP in dilute solutions of an unreactive solvent, benzene. (i) The rise of S_1 fluorescence excited at 397 nm is measurably faster (dominant component of 1.15 ps) than the decay of S_2 fluorescence (1.45 ps), an observation attributed to a contribution to the population of S_1 by a somewhat faster decay of the co-excited S_2' state. (ii) Two-photon excitation at 550 nm and subsequent relaxation of $S_{n > 2}$ produces a much higher ratio of $S_2':S_2$ populations than is produced by one-photon excitation at 397 nm, in the B(0,1) vibrational feature of the Soret band system. YBZ considered the possibility that their observations might be the result of a significant fraction of the $S_{n > 1}$ excited-state populations bypassing S_1 by radiationless relaxation but ruled this out on the basis of previous work²⁵ that appears to show that internal conversion to S_1 occurs with 100% efficiency. (We note, however, that this conclusion may be based on inaccurate data derived from experiments in which the effects of aggregation, reabsorption, and scattering have not been adequately accounted for, because the quantum yield of S_2-S_0 fluorescence reported in the same paper is a factor of 5 too small.) Moreover, the presence of an additional pathway that bypasses S_1 may remove all or part of a discrepancy, noted by YBZ, between the intensities of S_1-S_0 fluorescence excited by one photon at 397 nm vs two photons at 550 nm, attributed by

YBZ to significant two-photon absorption even when exciting with low laser power at 397 nm.

We offer an alternate interpretation of the data of YBZ that incorporates the results of the quantum yield measurements described above. First, we agree that a second excited state, S_2' , exists at approximately the same energy as S_2 , and that the one-photon absorption spectrum in the 370–450 nm region is a convolution of two transitions. We can now state, semiquantitatively, that the Soret band system consists of narrow features associated with the dominant, strong S_2-S_0 transition convoluted with considerably weaker, but broader absorption bands due to $S_2'-S_0$. At λ_{\max} in this region, the contribution to ϵ_{\max} of the former transition must outweigh that of the latter by at least 20:1, but on the red edge of the spectrum this ratio decreases by about a factor of 10, suggesting that the energy of the S_2' state may be slightly lower than that of S_2 , at least in ethanol. On the blue side of the maximum, the molar absorptivity of the $S_2'-S_0$ transition remains smaller than that of the B(0,1) feature of the S_2-S_0 transition but is relatively larger than it is at λ_{\max} . The population of S_2' (which is expected to be nonstatistically distributed among available vibrational states) would appear to relax by at least two parallel processes, one of which populates S_1 (at rates faster than from S_2), and one or more of which bypasses S_1 . The only reasonable possibilities for the latter process are $S_2'-S_0$ and $S_2'-T_n$. Two-photon excitation at 550 nm (YBZ) results in S_2' being populated preferentially by very fast (femtosecond) internal conversion from higher states, $S_{n>2}$, and then decaying independently of S_2 . These observations suggest not only that S_2' may be lower in energy than S_2 but also that the bound portion of its surface is displaced relative to that of S_2 and is only weakly coupled to it.

Conclusions

Zinc tetraphenylporphyrin in ethanol has been used as a model system to investigate the photophysics of the states accessed by one-photon excitation within the Soret and Q-bands under conditions where self-absorption of emission and solute aggregation are either eliminated or properly compensated. Under these conditions, the smallest S_2-S_0 Stokes shift yet measured, 115 cm^{-1} , and the largest S_2-S_0 absolute fluorescence quantum yield yet measured, 1.84×10^{-3} , are obtained. Accurate measurements of the relative quantum yields of S_2-S_0 to S_1-S_0 emission as a function of excitation wavelength reveal that a fast radiationless process that bypasses S_1 is operative among states accessed at excitation energies that span the full width of the Soret band. These data can be interpreted using the evidence of Yu, Baskin, and Zewail that a second excited state, S_2' , contributes a small fraction of the Soret band's integrated molar absorptivity and is responsible for an increasing fraction of photon absorption on both the red edge of the Soret band at $\lambda_{\text{ex}} > 430\text{ nm}$ and to the blue at $\lambda_{\text{ex}} < 409\text{ nm}$. The lifetimes of the S_2 and S_1 states have measured under similar conditions.

The values obtained confirm previous measurements and permit accurate evaluations of the rate constants for radiative and nonradiative decay of the excited S_1 and S_2 states.

Acknowledgment. We gratefully acknowledge the financial support of the State Committee for Scientific Research (KBN), Poland, project 4 T09A 166 24 and 4 T09A 152 25. R.P.S. is pleased to acknowledge the support of the Natural Sciences and Engineering Research Council of Canada. Dynamics studies were performed at the Centre for Ultrafast Laser Spectroscopy, A. Mickiewicz University, Poznan.

Note Added after ASAP Posting. This article was posted ASAP on 4/29/2004. The captions for Figures 1 and 2 have been interchanged. The correct version was posted on 5/7/2004.

References and Notes

- (1) Sternberg, E. D.; Dolphin, D.; Bruckner, C. *Tetrahedron* **1998**, *54*, 4151.
- (2) Lammi, R. K.; Ambrose, A.; Balasubramanian, T.; Wagner, R. W.; Bocian, D. F.; Holten, D.; Lindsey, J. S. *J. Am. Chem. Soc.* **2000**, *122*, 7579.
- (3) Mirkin, C. A.; Ratner, M. A. *Annu. Rev. Phys. Chem.* **1992**, *43*, 719.
- (4) Remacle, F.; Speiser, S.; Levine, R. D. *J. Phys. Chem. B* **2001**, *105*, 5589.
- (5) Van Patten, P. G.; Shreve, A. P.; Lindsey, J. S.; Donohoe, R. J. *J. Phys. Chem. B* **1998**, *102*, 4209.
- (6) Chosrowjan, H.; Taniguchi, S.; Okada, T.; Tagaki, S.; Arai, T.; Tokumaru, K. *Chem. Phys. Lett.* **1995**, *242*, 644.
- (7) Yu, H.-Z.; Baskin, S.; Zewail, A. H. *J. Phys. Chem. A* **2002**, *106*, 9845.
- (8) White, W. H. In *The Porphyrins*; Dolphin, D., Ed.; Academic Press: New York, 1978; Vol. 5, p 303.
- (9) Li, Y.; Steer, R. P. *Chem. Phys. Lett.* **2003**, *373*, 94.
- (10) Khairutdinov, R. F.; Serpone, N. *J. Phys. Chem.* **1995**, *99*, 11952.
- (11) Andersson, M.; Davidsson, J.; Hammarstrom, L.; Korppi-Tommola, J.; Peltola, T. *J. Phys. Chem. B* **1999**, *103*, 3258.
- (12) Gurzadyan, G. G.; Tran-Thi, T.-H.; Gustavsson, T. *J. Chem. Phys.* **1998**, *108*, 385.
- (13) Stehlmakh, G. F.; Tsvirko, M. P. A. C. S. *Symp. Ser.* **1986**, *321*, 118 and references therein.
- (14) Bajema, L.; Gouterman, M.; Rose, C. B. *J. Mol. Spectrosc.* **1971**, *39*, 421.
- (15) Tobita, S.; Kaizu, Y.; Kobayashi, H.; Tanaka, I. *J. Chem. Phys.* **1984**, *81*, 2962.
- (16) Mataga, N.; Shibata, Y.; Chosrowjan, H.; Yoshida, N.; Osuka, A. *J. Phys. Chem. B* **2000**, *104*, 4001.
- (17) Karolczak, J.; Komar, D.; Kubicki, T.; Wrozowa, T.; Dobek, K.; Ciesielska, B.; Maciejewski, A. *Chem. Phys. Lett.* **2001**, *344*, 154.
- (18) Demas, J. N.; Crosby, G. A. *J. Phys. Chem.* **1971**, *75*, 991.
- (19) Milewski, M.; Augustyniak, W.; Maciejewski, A. *J. Phys. Chem. A* **1998**, *102*, 7427.
- (20) Tsvirko, M. P.; Stehlmakh, G. F.; Pyatosin, V. E.; Solovyov, K. N.; Kachura, T. F. *Chem. Phys. Lett.* **1980**, *73*, 80.
- (21) Gradyushko, A. T.; Tsvirko, M. P. *Opt. Spektrosk.* **1971**, *31*, 548; *Opt. Spectrosc.* **1971**, *31*, 291.
- (22) Aaviksoo, J.; Frieberg, A.; Savikhin, S.; Stehlmakh, G. F.; Tsvirko, M. P. *Chem. Phys. Lett.* **1984**, *111*, 275 [quoting: Stehlmakh, G. F.; Tsvirko, M. P. *Zh. Prikl. Spektrosk.* **1983**, *39*, 428].
- (23) Tagaki, S.; Inoue, H. In *Molecular and Supramolecular Photochemistry*; Ramamurthy, V.; Schanze, K. S., Eds.; Marcel Dekker: New York, 2000; Vol. 5, p 215.
- (24) Strickler, S. J.; Berg, R. A. *J. Chem. Phys.* **1962**, *37*, 814.
- (25) Ohno, O.; Kaizu, Y.; Kobayashi, H. *J. Chem. Phys.* **1985**, *82*, 1779.